IOPscience iopscience.iop.org

Home Search Collections Journals About Contact us My IOPscience

Polar optical oscillations in quantum wires and free-standing wires: the electron-phonon interaction Hamiltonian

This article has been downloaded from IOPscience. Please scroll down to see the full text article.

1995 J. Phys.: Condens. Matter 7 1789

(http://iopscience.iop.org/0953-8984/7/9/006)

View the table of contents for this issue, or go to the journal homepage for more

Download details:
IP Address: 171.66.16.179
The article was downloaded on 13/05/2010 at 12:38

Please note that terms and conditions apply.

J. Phys.: Condens. Matter 7 (1995) 1789–1805. Printed in the UK

Polar optical oscillations in quantum wires and free-standing wires: the electron–phonon interaction Hamiltonian

F Comas†¶, A Cantarero‡+, C Trallero-Giner§ and M Moshinsky||

† Departamento de Física Aplicada, Universidad de Valencia, Dr Moliner 50, 46100 Burjasot, Valencia, Spain

‡ Max Planck Institut für Festkörperforschung, Heisenbergstrasse 1, 70569 Stuttgart, Germany

§ Department of Theoretical Physics, Havana University, Vedado 10400, Havana, Cuba

|| Instituto de Física, Universidad Autónoma de México, 20-364 México, 01000 DF, Mexico

Received 18 April 1994, in final form 19 October 1994

Abstract. By applying a phenomenological theory for long-wavelength polar optical oscillations to mesoscopic layered semiconductor structures, we calculate the normal modes of a quantum wire and of a free-standing wire. the cylindrical geometry is adopted with circular cross-section of radius r_0. The displacement field u and the electric potential ϕ are calculated for the different modes, as well as the dispersion relation curves. The case of the GaAs/AlAs structure is analysed. We limit ourselves to the study of oscillations perpendicular to the wire axis. The electron–phonon interaction Hamiltonian is derived for the present problem using the second-quantization formalism.

1. Introduction

Polar optical oscillations in mesoscopic layered semiconductor structures (quantum wells, superlattices, etc) have been intensively investigated in the last few years. [1, 2, 3, 4]. Oscillations for the long-wavelength limit are well known to be important in many physical problems and can be studied within the framework of phenomenological treatments such as the dielectric continuum model [5, 6, 7, 8, 9] or the hydrodynamic model [8, 10, 11, 12, 13]. An exhaustive analysis of the different phenomenological models has been reported in [8]. However, the application of these kinds of approach to mesoscopic structures led to a certain degree of disagreement with both Raman scattering experiments and calculations on the basis of microscopic models [14, 15, 16, 17, 18, 19, 20, 21]. Nevertheless, it has been proved that a rigorous application of the phenomenological theory, meeting all the requirements of macroscopic physics of continuous media, leads to results in close agreement with both experiments and microscopic calculations [22, 23]. The main points of this treatment are: (i) we should solve a system of coupled differential equations for the displacement field u and the electric potential ϕ; (ii) we should apply matching conditions at the interfaces in close consistency with both the differential equations of the treatment and the involved physical principles; (iii) we are in general led to coupled oscillation modes involving a mixed character. In the quantum well case we do not obtain uncoupled T (transversal), L

¶ On leave from Department of Theoretical Physics, Havana University, Vedado 10400, Havana, Cuba.

+ Permanent address: Departmento de Física Aplicada, Universidad de Valencia, 46100 Burjasot, Valencia, Spain.

0953-8984/95/091789+17$19.50 © 1995 IOP Publishing Ltd

(longitudinal) or interface modes. On the contrary, the modes can show predominantly T, L or interface character depending on the concrete physical conditions involved. All the above mentioned features of the modes follow in a natural manner when the coupled differential equations are properly solved and the appropriate matching conditions are applied. For further details [22, 23, 24] should be consulted.

The phenomenological theory of polar optical oscillations has been applied also to systems called quantum wires (QWs) and free-standing wires (FSWs). Preliminary results for the QW case have already been reported in [25]. It should be remarked that previous works related to QWs and FSWs (see, for instance, [26, 27, 28, 29, 30, 31, 35]) have usually incorporated the same kinds of difficulty discussed in the text above. The differences between such kinds of dielectric continuum approach and microscopic calculations were recently discussed by Rossi *et al* [36]. Microscopic calculations of the phonon dispersion for rectangular quantum wires embedded in AlAs have been reported in [32, 34, 36]. The anisotropic character of the phonon dispersion in that kind of structure was analysed for the first time in [32] and it is in accordance with similar calculations in quantum wells. Confined and interface (both GaAs and AlAs) phonons are studied in [36] where they conclude that the dielectric model with electrostatic boundary conditions is adequate, comparing with microscopic results, whenever the wave-vector is relevant for the electron–phonon scattering. Experimental evidence of surface phonons has been reported in [31], where a Raman scattering experiment has been carried out in GaAs cylindrical wires of 30 nm radius. The hydrodynamical model has been used in [27, 30, 35] to study the optical modes in wires of circular geometry. This kind of treatment considers the phonons as purely longitudinal or transverse, and the coupling between the electrostatic potential associated with the LO phonons and the mechanical vibrations is not taken into account. This model gives an incorrect formulation of the interface phonons and cannot reproduce the strong coupling between LO and TO phonons predicted by microscopic calculations [32, 36] and recently confirmed by a correct formulation of the phenomenological theory in quantum wells [17, 22] and superlattices [23]. In [26, 28, 33], the dielectric continuum model is applied to obtain the interface and confined modes in a quantum well with square symmetry. A critical analysis of the results of these works has been given in [29], where also interface phonons are analysed in different geometries (with different cross-sectional shapes). In the frame of the dielectric continuum model, the authors of [35] studied the optical modes and gave an extension *ad hoc* by using lattice dynamic theory and imposing that the electrostatic potential associated with the optical phonons and the displacement vector must vanish at the interfaces of the rectangular quantum wire.

The fundamental aim of the current work is to continue with the application of the model developed in [24] to QWs and FSWs. We have chosen a cylindrical geometry with circular cross-section of radius r_0 and also limited ourselves to the important case of oscillations perpendicular to the wire axis. Here we report the nature of the oscillation modes with detailed reference to the dispersion relation curves, the oscillation amplitudes and the electric potential. Moreover, a derivation of the Fröhlich-like electron–phonon interaction Hamiltonian by applying the standard methods of quantum field theory is presented. It is remarkable that the present calculations lead to a relatively close agreement with the microscopic calculations of [36].

2. Model and fundamental equations

We approach the present problem in the long-wavelength limit applying the physics of continuous media. For the description of the oscillations we use the displacement vector

field $\boldsymbol{u}$ (with units of length), which represents the relative displacement of the two ions involved (considering the typical cases of GaAs or AlAs). The other important quantity is the electric potential ϕ, related to the electric field $\boldsymbol{E}$ in the standard way $\boldsymbol{E} = -\nabla\phi$ for the unretarded limit ($c \to \infty$). Other physical parameters of the medium are: $\rho = (\bar{M}/v_c)$, the reduced mass density, $\bar{M}$ is the reduced mass of the ions and v_c is the unit cell volume; ω_T is the limiting (bulk) transverse optical frequency of the oscillations; β_L and β_T are two parameters describing the dispersion of the oscillations; ϵ_0 (ϵ_∞) are the static (optic) dielectric constants of the medium; ω_L is the limiting (bulk) longitudinal optical frequency of the oscillations, given by the Lyddane–Sachs–Teller relation: $\omega_L^2 = (\epsilon_0/\epsilon_\infty)\omega_T^2$. For the isotropic medium case the fundamental equations of this theory are [24, 25]

$$(\omega^2 - \omega_T^2)\boldsymbol{u} = \frac{\alpha}{\rho}\nabla\phi + \beta_L^2\nabla\nabla\cdot\boldsymbol{u} - \beta_T^2\nabla\times\nabla\times\boldsymbol{u} \tag{1}$$

and

$$\nabla^2\phi = \frac{4\pi\alpha}{\epsilon_\infty}\nabla\cdot\boldsymbol{u} \tag{2}$$

where

$$\alpha^2 = (\epsilon_0 - \epsilon_\infty)\rho\omega_T^2/4\pi. \tag{3}$$

The matching boundary conditions were also derived rigorously from equations (1) and (2) (see [25]) and bear a direct physical meaning. They are:

(i) continuity of $\boldsymbol{u}$ and ϕ at the interfaces;

(ii) continuity at the interfaces of σ_N, where:

$$\sigma_N = \sigma\cdot N \tag{4}$$

N being a unit vector normal to the interface and σ a tensor, which follows from (1), whose components are given by:

$$\sigma_{ij} = -\rho(\beta_L^2 - 2\beta_T^2)(\nabla\cdot u)\delta_{ij} - 2\rho\beta_T^2 u_{ij} \tag{5}$$

(iii) continuity at the interfaces of $D_N = \boldsymbol{D}\cdot\boldsymbol{N}$, where $\boldsymbol{D}$ is the electric induction vector, given by:

$$\boldsymbol{D} = 4\pi\alpha\boldsymbol{u} - \epsilon_\infty\nabla\phi. \tag{6}$$

In the current work all the equations given above will be applied to a QW (or to an FSW) of cylindrical shape. Then the z axis is chosen as the cylinder axis with infinite length. The cylinder cross-section is circular with radius r_0. In the QW case for $r < r_0$ we have a certain medium (say GaAs) and for $r > r_0$ the medium is different (say, AlAs). In the FSW case for $r > r_0$ we have just vacuum or some other medium (such as quartz) allowing free oscillations of the surface. For this kind of structures we shall use cylindrical coordinates (r, θ, z). Equations (1) and (2) represent a complicated system of coupled differential equations. For their solution we make use of auxiliary potentials ψ and $\boldsymbol{A}$, such that:

$$\boldsymbol{u} = \nabla\psi + \nabla\times\boldsymbol{A} \tag{7}$$

where the supplementary condition $\nabla\cdot\boldsymbol{A} = 0$ is imposed. Substitution of (7) in (1) leads us to a certain vector equation. Taking the divergence and the curl of such an equation (and also applying equation (2)) it can be proved, after a little algebra, that the auxiliary potentials satisfy the following equations:

$$\nabla^2\left[\nabla^2\boldsymbol{A} + \frac{\omega_T^2 - \omega^2}{\beta_T^2}\boldsymbol{A}\right] = 0 \tag{8}$$

and

$$\nabla^2\left[\nabla^2\psi + \frac{\omega_L^2 - \omega^2}{\beta_L^2}\psi\right] = 0. \tag{9}$$

Equations (8) and (9) are uncoupled equations for A and ψ, which can be solved applying straightforward methods. Once we have obtained solutions for (8) and (9), we obtain u by means of equation (7). Substitution of this explicit expression for u in equation (2) allows us to determine the electric potential ϕ after solution of the resulting Poisson equation. By this procedure we obtain general analytical solutions for the coupled quantities u and ϕ. In the frame of the present work we shall limit ourselves to the investigation of oscillations perpendicular to the wire axis, i.e., $q_z = 0$ (and hence $u_z = 0$), where q is the wavevector. We are thus considering a particular case, which, however, entails a direct interest for the study of certain physical processes (one-phonon resonant Raman scattering for several scattering configurations [37], for instance) and gives us an insight into the nature of the oscillations. The following results obtained cannot be used for a direct evaluation of physical processes such as scattering rates or free carrier absorption, where $q_z \neq 0$. For $u_z = 0$ we can take:

$$A = A_z(r, \theta)\hat{z} \tag{10}$$

where $\hat{z}$ is the unit vector along the z axis. Taking also $\psi = \psi(r, \theta)$ we are led to a displacement vector of the form:

$$u = u_r(r, \theta)\hat{r} + u_\theta(r, \theta)\hat{\theta} \tag{11}$$

where $\hat{r}$ and $\hat{\theta}$ are the corresponding unit vectors in cylindrical coordinates. It can be easily seen that:

$$u_r = \frac{\partial\psi}{\partial r} + \frac{1}{r}\frac{\partial A_z}{\partial\theta} \qquad u_\theta = \frac{1}{r}\frac{\partial\psi}{\partial\theta} - \frac{\partial A_z}{\partial r} \tag{12}$$

while A_z and ψ satisfy the following equations:

$$\frac{1}{r}\frac{\partial}{\partial r}\left(r\frac{\partial A_z}{\partial r}\right) + \frac{1}{r^2}\frac{\partial^2 A_z}{\partial\theta^2} + \frac{\omega_T^2 - \omega^2}{\beta_T^2}A_z = f_1 \tag{13}$$

$$\frac{1}{r}\frac{\partial}{\partial r}\left(r\frac{\partial\psi}{\partial r}\right) + \frac{1}{r^2}\frac{\partial^2\psi}{\partial\theta^2} + \frac{\omega_L^2 - \omega^2}{\beta_L^2}\psi = f_2. \tag{14}$$

In equations (13) and (14) the functions f_1 and f_2 are solutions of the Laplace equation in cylindrical coordinates:

$$\nabla^2 f_i = 0. \tag{15}$$

We should require the solutions to be regular in $r = 0$ and in $r = \infty$. We will not present here the tedious (but straightforward) mathematical details, and will just report the final results. A general analytical basis for the solution space of this class of problems is:

$$\begin{bmatrix} (in/r)f_n(Qr) \\ -Qf_n'(Qr) \\ 0 \end{bmatrix} e^{in\theta} \qquad \begin{bmatrix} qf_n'(qr) \\ (in/r)f_n(qr) \\ (4\pi\alpha/\epsilon_\infty)f_n(qr) \end{bmatrix} e^{in\theta}$$
$$\begin{bmatrix} [n\alpha/\rho(\omega^2 - \omega_T^2)]r^{n-1} \\ [in\alpha/\rho(\omega^2 - \omega_T^2)]r^{n-1} \\ r^n \end{bmatrix} e^{in\theta} \qquad \begin{bmatrix} -[n\alpha/\rho(\omega^2 - \omega_T^2)]r^{-(n+1)} \\ [in\alpha/\rho(\omega^2 - \omega_T^2)]r^{-(n+1)} \\ r^{-n} \end{bmatrix} e^{in\theta}. \tag{16}$$

An arbitrary solution of the equations (1) and (2) within the conditions of the present problem can be represented as a linear combination of the vectors given in (16). For the

determination of the solution in a given region divergent vectors in some point of that region should be excluded. We have also introduced:

$$q^2 = \frac{\omega_L^2 - \omega^2}{\beta_L^2} \qquad Q^2 = \frac{\omega_T^2 - \omega^2}{\beta_T^2} \tag{17}$$

and $f_n(x)$ represents a solution of the Bessel equation of order n (this function should be bounded in its domain of definition). It must be noticed that $\omega < \omega_L$ for all the frequencies involved in the present problem; thus q is always a real quantity. On the contrary, Q is real for $\omega < \omega_T$, but it is an imaginary quantity for $\omega_T < \omega < \omega_L$.

We must determine the vector σ_N, defined in (4), in cylindrical coordinates. An elementary evaluation of this vector leads to the following result:

$$\sigma_N = \sigma_r \hat{r} + \sigma_\theta \hat{\theta} + \sigma_z \hat{z} \tag{18}$$

where

$$\begin{aligned}
\sigma_r &= -\rho\beta_L^2 \frac{\partial u_r}{\partial r} - \rho(\beta_L^2 - 2\beta_T^2)\left(\frac{\partial u_z}{\partial z} + \frac{1}{r}\frac{\partial u_\theta}{\partial \theta} + \frac{1}{r}u_r\right) \\
\sigma_\theta &= -\rho\beta_T^2\left(\frac{\partial u_\theta}{\partial r} + \frac{1}{r}\frac{\partial u_r}{\partial \theta} - \frac{1}{r}u_\theta\right) \\
\sigma_z &= -\rho\beta_T^2\left(\frac{\partial u_r}{\partial z} + \frac{\partial u_z}{\partial r}\right).
\end{aligned} \tag{19}$$

3. Quantum wire and free-standing wire

Let us now assume a cylindrical QW with GaAs for $r < r_0$ and AlAs for $r > r_0$. Instead of the general matching boundary conditions depicted in section 2, in this case we shall impose [22]

(i) continuity of ϕ and D_N at $r = r_0$ ($D_N \equiv D_r = 4\pi\alpha u_r - \epsilon_\infty \partial\phi/\partial r$)
(ii) $u = 0$ for $r = r_0$.

The matching conditions described above should be applied to the solutions of the QW case. Avoiding mathematical details, we just report the results obtained [38]:

$$\begin{aligned}
u_r = B\Bigg\{ &\frac{n f_{n+1}(x)}{y f_{n+1}(y)} \frac{r_0}{r} f_n\left(y\frac{r}{r_0}\right) + f_n'\left(x\frac{r}{r_0}\right) \\
&+ \frac{\epsilon_{a\infty}}{\epsilon_{b\infty} + \epsilon_{a\infty}} \left(\frac{\beta_L}{\beta_T}\right)^2 \frac{R^2}{y^2}\left[f_{n-1}(x) + \frac{n}{x} f_n(x)\left(\frac{\epsilon_{b\infty}}{\epsilon_{a\infty}} - 1\right)\right]\left(\frac{r}{r_0}\right)^{n-1}\Bigg\} e^{in\theta}
\end{aligned} \tag{20}$$

$$\begin{aligned}
u_\theta = B\Bigg\{ &\frac{f_{n+1}(x)}{f_{n+1}(y)} f_n'\left(y\frac{r}{r_0}\right) + \frac{n}{x}\left(\frac{r_0}{r}\right) f_n\left(x\frac{r}{r_0}\right) \\
&+ \frac{\epsilon_{a\infty}}{\epsilon_{b\infty} + \epsilon_{a\infty}} \left(\frac{\beta_L}{\beta_T}\right)^2 \frac{R^2}{y^2}\left[f_{n-1}(x)\right. \\
&\left. + \frac{n}{x} f_n(x)\left(\frac{\epsilon_{b\infty}}{\epsilon_{a\infty}} - 1\right)\right]\left(\frac{r}{r_0}\right)^{n-1}\Bigg\} e^{i(n\theta + \pi/2)}
\end{aligned} \tag{21}$$

$$\phi = \frac{4\pi\alpha}{\epsilon_{a\infty}}\frac{B}{q}\begin{cases} \{f_n(xr/r_0) - (x/n)[\epsilon_{a\infty}/(\epsilon_{b\infty}+\epsilon_{a\infty})] \\ \times\left[f_{n-1}(x) + n/xf_n(x)\,(\epsilon_{b\infty}/\epsilon_{a\infty} - 1)\right]\}(r/r_0)^n\,e^{in\theta} & r < r_0 \\ \{f_n(x) - (x/n)[\epsilon_{a\infty}/(\epsilon_{b\infty}+\epsilon_{a\infty})] \\ \times\left[f_{n-1}(x) + n/xf_n(x)\,(\epsilon_{b\infty}/\epsilon_{a\infty} - 1)\right]\}(r_0/r)^n\,e^{in\theta} & r > r_0. \end{cases} \tag{22}$$

In the expressions above: $x = qr_0$, $y = Qr_0$ and

$$\left(\frac{r_0}{\beta_L}\right)^2(\omega_L^2 - \omega_T^2) = R^2 = x^2 - \left(\frac{\beta_T}{\beta_L}\right)^2 y^2 \tag{23}$$

while the constant B was introduced in order to ensure the normalization of the oscillation modes. The eigenfrequencies of the oscillation modes for this case are reported in [25]. For an FSW we have $u = 0$ for $r > r_0$ but there is an electric potential $\phi \neq 0$ in the whole space. The form of the solutions can be easily deduced from the general analytic basis studied in section 2. The matching boundary conditions corresponding to the present case are:

(i) continuity of ϕ at $r = r_0$
(ii) $\sigma_N = 0$ at $r = r_0$
(iii) continuity of $D_N \equiv D_r$ at $r = r_0$.

The latter condition entails the following relation:

$$4\pi\alpha u_r(r_0^-, \theta) - \epsilon_{a\infty}\frac{\partial\phi}{\partial r}(r_0^-, \theta) = -\epsilon_{b\infty}\frac{\partial\phi}{\partial r}(r_0^+, \theta). \tag{24}$$

Applying the above mentioned matching boundary conditions, we are led to the following solution of our problem:

$$u_r = B\frac{1}{r_0}\left[-\frac{n}{y^2}\frac{g_n(x)}{f_{n+2}(y)}\frac{r_0}{r}f_n\left(y\frac{r}{r_0}\right) + xf_n'\left(x\frac{r}{r_0}\right) + n\left(\frac{\beta_L^2}{\beta_T^2}x^2 - y^2\right)t_n(x, y)\left(\frac{r}{r_0}\right)^{n-1}\right]e^{in\theta} \tag{25}$$

$$u_\theta = B\frac{1}{r_0}\left[-\frac{1}{y}\frac{g_n(x)}{f_{n+2}(y)}f_n'\left(y\frac{r}{r_0}\right) + n\left(\frac{r_0}{r}\right)f_n\left(x\frac{r}{r_0}\right) + n\left(\frac{\beta_L^2}{\beta_T^2}x^2 - y^2\right)t_n(x, y)\left(\frac{r}{r_0}\right)^{n-1}\right]e^{i(n\theta+\pi/2)} \tag{26}$$

$$\phi = \frac{4\pi\alpha}{\epsilon_{a\infty}}B\begin{cases}\left[f_n(xr/r_0) - t_n(x, y)\,(r/r_0)^n\right]e^{in\theta} & r < r_0 \\ \left[f_n(x) - t_n(x, y)\right](r_0/r)^n\,e^{in\theta} & r > r_0\end{cases} \tag{27}$$

where

$$t_n(x, y) = \left[y^2 f_n(x) f_{n+2}(y) + \frac{\epsilon_{a\infty}}{\epsilon_{b\infty}}g_n(x)f_n(y)\right]\left[\left(\frac{\epsilon_{a\infty}}{\epsilon_{b\infty}}\left(\frac{\beta_L}{\beta_T}\right)^2 x^2 + y^2\right)f_{n+2}(y)\right]^{-1} \tag{28}$$

and

$$g_n(x) = \frac{\beta_L^2}{\beta_T^2}x^2 f_n(x) - 2(n+1)xf_{n+1}(x) \tag{29}$$

B is again a normalization constant. The eigenfrequencies of the oscillations for the FSW case are given by solving the following secular equation:

$$2n(n-1)\left(\frac{\beta_L^2}{\beta_T^2}\right)R^2 t_n(x,y)f_{n+2}(y) + 2ny^2 f_{n+2}(y)\left[xf_n'(x) - f_n(x)\right] + g_n(x)\left[2yf_n'(y) + (y^2 - 2n^2)f_n(y)\right] = 0 \tag{30}$$

where R was defined in equation (23).

4. Electron–phonon interaction Hamiltonian

The fundamental equations of this theory are equations (1) and (2), having the general form:

$$\mathcal{M}\begin{bmatrix} u_m \\ \phi_m \end{bmatrix} = \omega_m{}^2 \begin{bmatrix} \mathbf{I} & \mathbf{0} \\ \mathbf{0} & \mathbf{0} \end{bmatrix}\begin{bmatrix} u_m \\ \phi_m \end{bmatrix} \tag{31}$$

where $\mathcal{M}$ is a matrix differential operator [39]. We use subscript m to label the different eigenvalues. Elsewhere [39] we have proved that: (i) the operator $\mathcal{M}$ is Hermitian with respect to the solution space of the present problem; (ii) the eigensolutions of equation (31) are orthogonal in the following sense (see the appendix):

$$\int \rho u_m^* \cdot u_{m'}\, \mathrm{d}^3 r = 0 \qquad \text{for } m \neq m'. \tag{32}$$

The integral in (32) is taken over the whole volume of the system. For a Hermitian operator it is clear that the set of eigensolutions of equation (31) (i.e., the infinite set of eigenvectors u_m) constitute a complete set. Therefore, from the eigensolutions of equation (31) we can always construct a complete set of orthonormal eigenvectors, representing a basis that spans the solution space of the present problem. It has been shown in [8] that the electron–phonon scattering rates in quantum wells are practically independent of the set of functions used, if this set is orthogonal and complete. In [39] the necessary and sufficient conditions to have a space of orthonormal and complete functions independent of the geometry of the system has been given. These conditions are connected to the Hermiticity of the operator $\mathcal{M}$ and the boundary conditions that the functions u and ϕ have to satisfy.

For our case we introduce the following labelling of the eigenvectors:

$$u_{nm}(r,\theta) = \left\{R_{nm}(r)\hat{r} + \Theta_{nm}(r)\hat{\theta}\right\}\frac{\mathrm{e}^{in\theta}}{\sqrt{2\pi}}. \tag{33}$$

The functions $R_{nm}(r)$ and $\Theta_{nm}(r)$ can be easily inferred from the results of section 2. The orthonormality condition is then given as follows

$$\int \rho\left[R_{nm}^* R_{nm'} + \Theta_{nm}^*\Theta_{nm'}\right] r\, \mathrm{d}r = \delta_{mm'}. \tag{34}$$

The other important point is completeness, which can be stated as follows:

$$\sum_{n,m} \rho\left[R_{nm}^*(r)R_{nm}(r') + \Theta_{nm}^*(r)\Theta_{nm}(r')\right]\mathrm{e}^{in(\theta-\theta')} = 2\pi\frac{\delta(r-r')}{r}\delta(\theta-\theta'). \tag{35}$$

It is also clear that the potential ϕ can be written in the form:

$$\phi_{nm}(r,\theta) = f_{nm}(r)\mathrm{e}^{in\theta}. \tag{36}$$

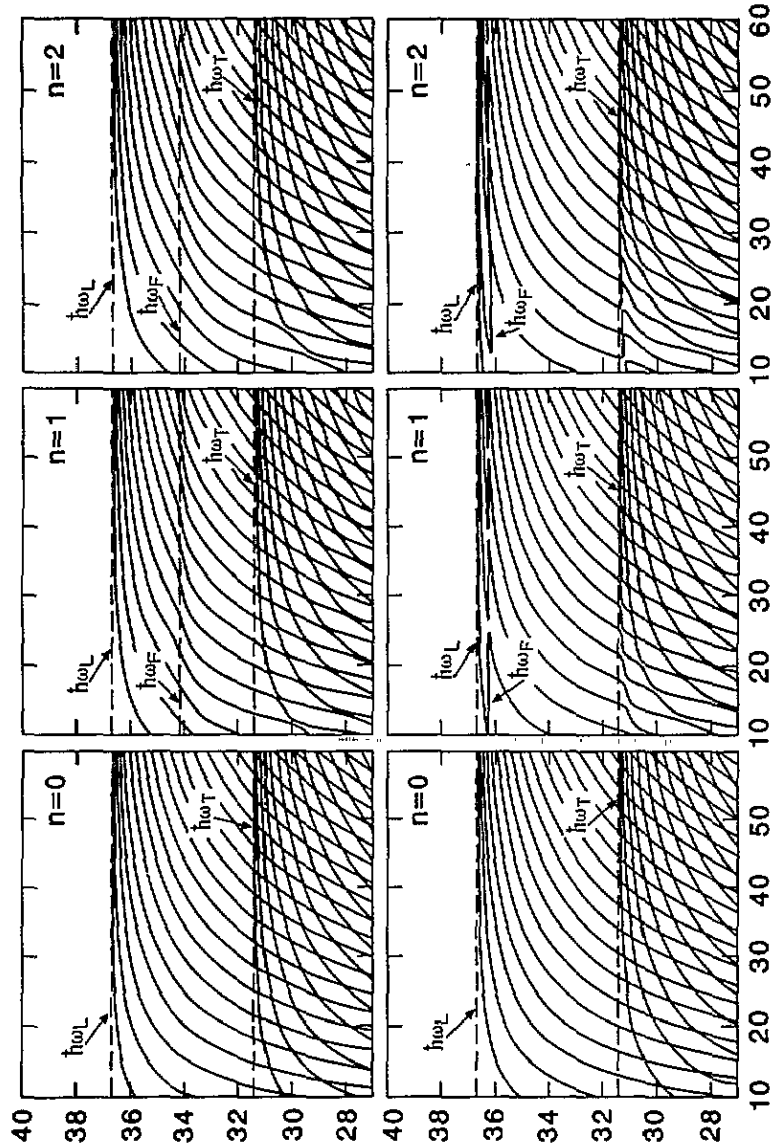

Figure 1. Dispersion relation curves as a function of the wire radius r_0 for three different values of n ($n = 0$, 1 and 2). The upper curves correspond to the QW case, while the lower ones correspond to the FWS. The dashed lines correspond to the longitudinal and transverse optical frequencies. Also the Fröhlich frequency is indicated (see text).

From the eigenvectors obtained in the previous sections we can construct a general displacement vector $u(r, \theta, t)$ by linear superposition. In a similar way we can construct a general potential $\phi(r, \theta, t)$. In the second-quantization formalism, the components of $\hat{u}(r, t)$, in cylindrical coordinates, are given by:

$$\hat{u}_r = \sum_{n,m} C_{nm} \left[R_{nm}(r) e^{i(n\theta - \omega t)} \hat{b}_{nm} + \text{HC} \right] \tag{37}$$

$$\hat{u}_\theta = \sum_{n,m} C_{nm} \left[\Theta_{nm}(r) e^{i(n\theta - \omega t)} \hat{b}_{nm} + \text{HC} \right]. \tag{38}$$

Notice that, without loss of generality, we assume constants C_{nm} to be real quantities. Following the procedure described in [39], the constants C_{nm} are determined. We here write just the final result:

$$C_{nm} = \left[\frac{\hbar}{2\omega_{nm} L} \right]^{1/2}. \tag{39}$$

We thus have a complete determination of the quantum field operators describing the polar optical phonons in the structures we are studying. In order to determine the electron–phonon interaction Hamiltonian we have to write the corresponding operator for the potential:

$$\hat{\phi}(r, \theta, t) = \sum_{n,m} C_{nm} \frac{4\pi\alpha r_0}{\epsilon_\infty} \left[F_{nm}(r) e^{i(n\theta - \omega t)} \hat{b}_{nm} + \text{HC} \right]. \tag{40}$$

The constants C_{nm} must be the same as in (37) and in (38) because these quantities correspond to solutions of the coupled equations of this theory. $F_{nm}(r)$ is defined by:

$$f_{nm}(r) = \frac{4\pi\alpha r_0}{\epsilon_\infty} F_{nm}(r) \tag{41}$$

where $f_{nm}(r)$ was introduced in (36). We are thus finally led to a Fröhlich-like electron–phonon interaction Hamiltonian, which can be obtained from $-e\hat{\phi}$:

$$\hat{\mathcal{H}} = \sum_{n,m} \tilde{C}_{nm} \left[F_{nm}(r) e^{in\theta} \hat{b}_{nm} + \text{HC} \right] \tag{42}$$

where

$$\tilde{C}_{nm} = \left[\frac{\pi\omega_L \rho}{\omega_{nm}} \right]^{1/2} r_0^2 c_F \qquad c_F = -\sqrt{\frac{2\pi e^2 \hbar \omega_L}{V} (\epsilon_{a\infty}^{-1} - \epsilon_{a0}^{-1})}. \tag{43}$$

It should be also remarked that when writing the Hamiltonian $t = 0$ was set. Concerning functions $F_{nm}(r)$, they have different forms for the QW and for the FSW. From equation (22) we have:

$$F_{nm}^{QW} = B_{nm} \begin{cases} (1/x) f_n(xr/r_0) - s_n(x) (r/r_0)^n & r < r_0 \\ \left[(1/x) f_n(x) - s_n(x) \right] (r_0/r)^n & r > r_0 \end{cases} \tag{44}$$

where

$$s_n(x) = \frac{\epsilon_{a\infty}}{\epsilon_{a\infty} + \epsilon_{b\infty}} \left[\frac{1}{n} f_{n-1}(x) + \frac{1}{x} \left(\frac{\epsilon_{b\infty} - \epsilon_{a\infty}}{\epsilon_{a\infty}} \right) f_n(x) \right]. \tag{45}$$

From equation (27) we have:

$$F_{nm}^{FSW} = B_{nm} \begin{cases} f_n(xr/r_0) - t_n(x, y) (r/r_0)^n & r < r_0 \\ \left[f_n(x) - t_n(x, y) \right] (r_0/r)^n & r > r_0 \end{cases} \tag{46}$$

where $t_n(x, y)$ was defined in (28). It should be noted that in equations (44) and (46) the constants B_{nm} are the same as introduced in section 3 in order to ensure the orthonormality of the eigenvectors u_{nm}, i.e., equation (34). The Hamiltonians (44) and (46) are reduced to those obtained in the dielectric continuum model for a sufficiently large r_0. Purely superficial modes are obtained for $r_0 \to \infty$, i.e. when the mechanical boundary conditions (short-range interactions) are negligible. In that case, the long-range interactions associated with the electrostatic potential are dominant. Thus, our phenomenological model is reduced to the dielectric continuum model with electrodynamical boundary conditions as a limiting case. If r_0 is smaller than or of the order of q^{-1} and Q^{-1}, the effects of the mechanical boundary conditions become important. In the general case $q_z \neq 0$ the above discussion still remains valid. We have thus completely determined the electron–phonon interaction Hamiltonian $\hat{\mathcal{H}}$, describing the Fröhlich-like interaction between electrons and polar optical phonons in the studied structures. It must be remembered that, within the restrictions of our calculations, this Hamiltonian describes the interaction with phonons having $q_z = 0$.

5. Numerical results

For a numerical analysis of the results of sections 3 and 4 we have taken the parameters of GaAs [22]. The study of the QW has been carried out within the simplified assumption $\epsilon_{a\infty} = \epsilon_{b\infty}$, but for the FSW $\epsilon_{b\infty}$=1. Figure 1 shows dispersion relation curves (phonon energies $\hbar\omega$ as a function of radius r_0) for three values of n: $n = 0$, $n = 1$ and $n = 2$. The three graphs of the upper part of the figure correspond to the QW case, while the three graphs of the lower part correspond to the FSW case. For $n = 0$ we have decoupled L and T modes. The broken lines correspond to the bulk L and T phonon energies respectively. For $n \neq 0$ the modes are coupled and there can be seen the strong mixing between the T and L parts of the oscillations. It is also seen that, whenever a curve resembling an L decoupled phonon dispersion curve approaches the corresponding nearly 'T phonon' curve an anticrossing takes place and their behaviour changes from L to T phonon dispersion and vice versa. At these points of strong dispersion the contribution from the electric part of the oscillations is stronger. These results agree qualitatively well with those obtained in the microscopic calculations of [32, 36] for a QW with rectangular cross-section. The strong mixing between T and L phonons has been predicted by microscopic models (see for instance [15]) and correctly described by phenomenological continuum treatments in QW [22, 23]. As $r_0 \to \infty$ the bulk T and L phonon dispersion relations are recovered. It is interesting to realize that, in the $n \neq 0$ case, a new solution appears between $\hbar\omega_L$ and $\hbar\omega_T$, which correspond to a homogeneous polarization of the cylinder. This is the so called Fröhlich frequency, $\hbar\omega_F$, which appears from the boundary conditions in finite media, and it was introduced by Fröhlich in the study of spheres embeded in an infinite medium [40, 41]. For that frequency, there is no difference between longitudinal and transverse modes. In the case of a cylinder, it can be written as:

$$\omega_F^2 = \frac{\epsilon_{a0} + \epsilon_{b\infty}}{\epsilon_{a\infty} + \epsilon_{b\infty}} \omega_T^2 \tag{47}$$

and, substituting the parameters of GaAs, $\hbar\omega_F = 36.28$ meV for the QW case and $\hbar\omega_F = 34.15$ meV for the FSW. Figure 2 shows the components of the displacement vector u as a function of r for the FSW case. The drawings are the first and second solutions for a radius of $r_0 = 21.5$ Å for three different values of n ($n = 0$, 1 and 2). The solid curve corresponds to the u_r component, while the dashed line corresponds to the u_θ solution, which vanishes in the $n = 0$ case (if the vibrations correspond to transverse solutions, the component of

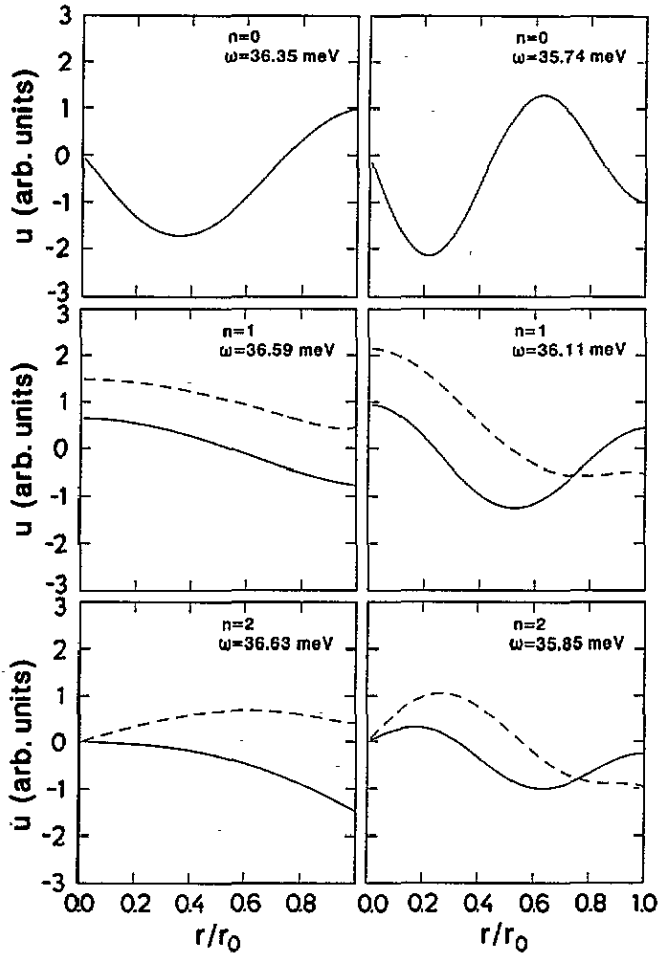

Figure 2. Phonon amplitudes $R_{nm}(r,\theta)$ (solid line) and $\Theta_{nm}(r)$ (dashed line) as a function of r ($m = 1$, 2 and 3; $n = 0$, 1 and 2) for the FSW case. In the $n = 0$ case we show only the $R_{nm}(r)$ component, since $\Theta_{nm}(r,\theta) = 0$ for the first longitudinal mode. The calculations correspond to a radius $r_0 = 21.5$. The amplitude has been normalized to the section of the cylinder, following equation (34). The same arbitrary units are used in all figures.

u different from zero is u_θ). The amplitude in the surface can be different from zero because the boundary conditions are applied over the stress component ($\sigma_N = 0$ at the surface). For the description of the potential we are using both direct plots of ϕ against r and tridimensional plots. In figure 3 there are shown such plots for the FSW case. We also present the $n = 0$, 1 and 2 modes for different phonon energies. In the tridimensional plots we use variables x and y, which should not be confused with the x and y variables used in previous sections. In this case they represent usual cartesian coordinates, related to the cylindrical coordinates in the usual way: $x = r\cos\theta$ and $y = r\sin\theta$. Moreover, x and y are measured in units of r_0. The potential profiles were taken at $x = 0$, while ϕ was measured in units of:

$$\phi_0 = -\frac{c_F}{e}\sqrt{\frac{\hbar\omega}{V}}.$$

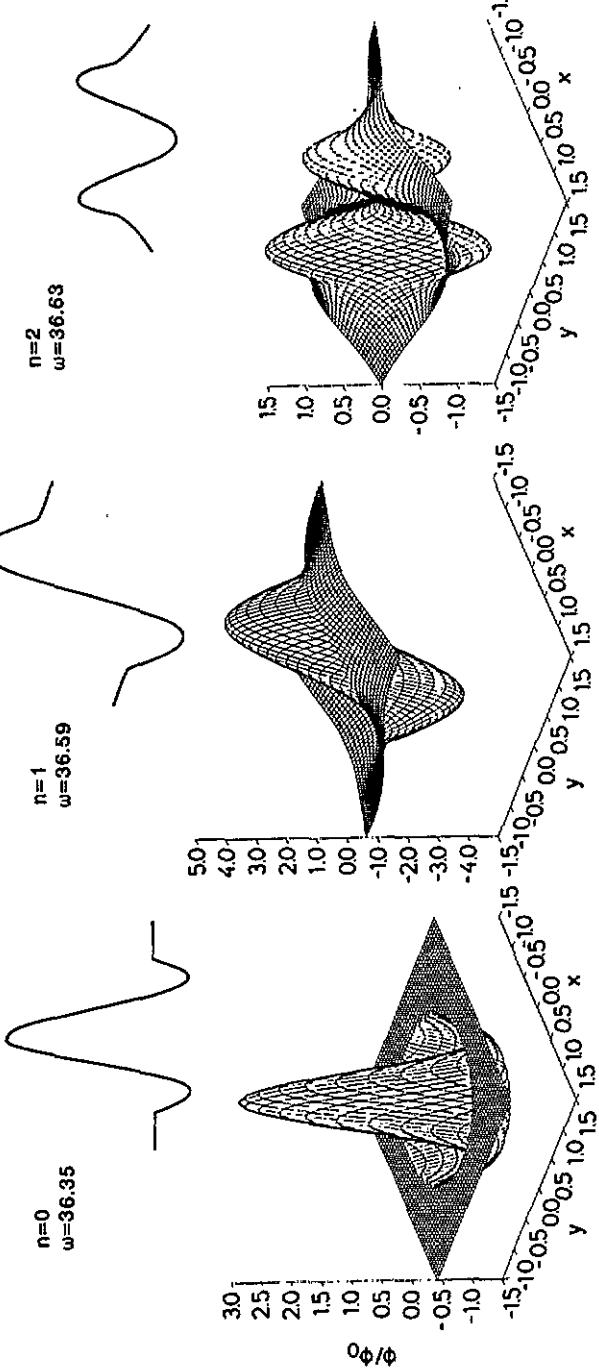

Figure 3. Two-dimensional plots of the electrostatic potential $\phi_{nm}(r, \theta)$ as a function of r and θ for $n = 0$, 1 and 2 ($m = 1$). x and y represent standard Cartesian coordinates. The profiles in the $x = 0$ plane are also shown. The potential has been divided by the constant $\sqrt{2\pi\hbar^2\omega_{LO}^2(\epsilon_\infty^{-1} - \epsilon_0^{-1})/V}$, and has units of meV$^{-1/2}$ Å.

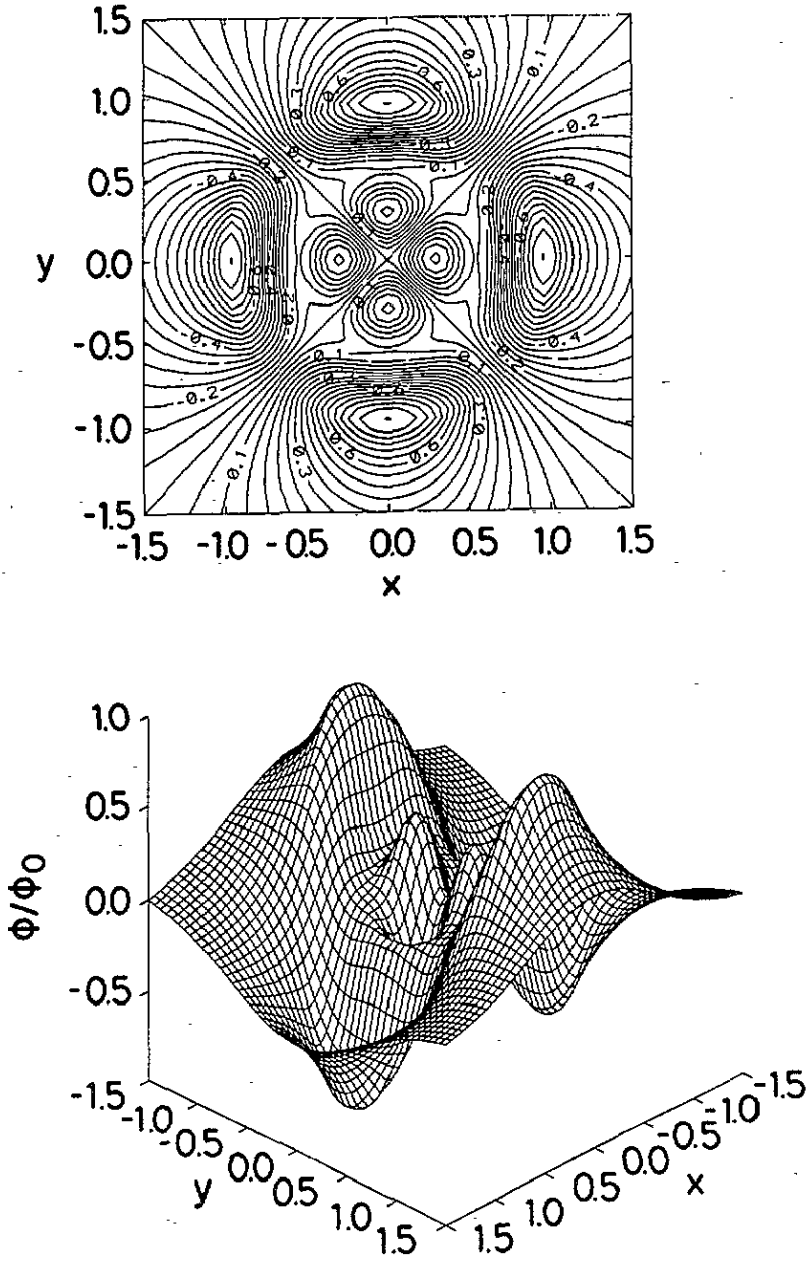

Figure 4. Electrostatic potential $\phi_{nm}(r, \theta)$ as a function of r and θ for $n = m = 2$. x and y represent standard Cartesian coordinates. At the top we show the projection on the $z = 0$ plane, and at the bottom a three-dimensional plot. The potential has been divided by the constant $\sqrt{2\pi\hbar^2\omega_{LO}^2(\epsilon_\infty^{-1} - \epsilon_0^{-1})/V}$, and has units of meV$^{-1/2}$ Å.

We can observe in the potential profile (at the top of figure 3) the continuity of the potential at $r = r_0$. Finally, figure 4 shows another graph for the potential in the form of equipotential curves in the (x, y) plane (top) and as a three-dimensional plot (bottom). The

mode with $n = 2$ and $m = 2$ is presented. The modes were all normalized in the form described in section 3. It can be seen that we obtain the correct symmetry pattern for the potential and the mechanical oscillation amplitudes. It is also obvious that the requirements of classical electrodynamics are fulfilled.

6. Concluding remarks

In this work we aimed to give a relatively complete treatment of the polar optical phonons and the electron–phonon interaction in semiconductor structures of the type of QWs and FSWs having cylindrical geometry. We studied the important case of axial wave vector q_z equal to zero. Our treatment is characterized by a consistent application of the phenomenological approach, based on the principles of macroscopic physics of continuous media. We have proved that such a treatment, including a correct manipulation of the matching problem, leads to results that (i) do not violate the standard principles of macroscopic physics, (ii) provide a satisfactory account of the physical features of the eigenmodes in a QW and an FSW, and also appear to agree well with microscopic calculations. Therefore, artificially *ad hoc* manipulations are not needed in order to get correct results and we also do not have to induce the correct long-wavelength behaviour starting from microscopic models.

Acknowledgments

The authors wish to thank Professor Manuel Cardona for valuable discussions and Dr M P Chamberlain for a critical reading of the manuscript. We would like to thank the University of Valencia and the University of Havana for stimulating the cooperation. One of us (AC) thanks the Ministerio de Educación y Ciencia of Spain for financial support and the Max Planck Institute for hospitality. This work was partially supported by Grant PB92-1076 of the DGICYT of the Ministerio de Educación of Spain.

Appendix. Orthogonality of the amplitudes

Let us now briefly describe how the orthogonality condition (i.e., equation (32)) can be proved in our case. From equations (1) and (2), taking due account of equations (33) and (36), we can find that

$$\left[\omega_m^2 - \omega_T^2 + (n^2\beta_T^2 + \beta_L^2)\frac{1}{r^2}\right] R_m = \frac{\alpha}{\rho} f_m' + \beta_L^2 R_m'' + \frac{\beta_L^2}{r} R_m' + \frac{in}{r}(\beta_L^2 - \beta_T^2)\Theta_m - \frac{in}{r^2}(\beta_L^2 + \beta_T^2)\Theta_m \tag{A1}$$

$$\left[\omega_m^2 - \omega_T^2 + (n^2\beta_L^2 + \beta_T^2)\frac{1}{r^2}\right] \Theta_m = \frac{in\alpha}{\rho r} f_m + \beta_T^2 \Theta_m'' + \frac{\beta_T^2}{r}\Theta_m' + \frac{in}{r}(\beta_L^2 - \beta_T^2) R_m' + \frac{in}{r^2}(\beta_L^2 + \beta_T^2) R_m. \tag{A2}$$

For brevity we are avoiding the subscript n in all our expressions. We now proceed in a rather standard way for this kind of demonstration. (A1) is multiplied by R_m^*. After that

we take the complex conjugate of equation (A1) with the change $m \to m'$ and multiply it by R_m. Subtracting the second equation from the first one we obtain:

$$(\omega_m^2 - \omega_{m'}^2)R_{m'}^* R_m = \frac{\alpha}{\rho}(R_{m'}^* f_m' - R_m f_{m'}'^*) + \beta_L^2(R_m'' R_{m'}^* - R_{m'}''^* R_m) + \frac{\beta_L^2}{r}(R_m' R_{m'}^* - R_m R_{m'}'^*) + \frac{in}{r}(\beta_L^2 - \beta_T^2)[R_{m'}^* \Theta_{m'}' + R_m \Theta_{m'}'^*] - \frac{in}{r^2}(\beta_L^2 + \beta_T^2)[R_{m'}^* \Theta_m + \Theta_{m'}^* R_m]. \tag{A3}$$

Applying the same procedure to equation (A2) we obtain:

$$(\omega_m^2 - \omega_{m'}^2)\Theta_{m'}^* \Theta_m = \frac{in\alpha}{\rho r}(\Theta_{m'}^* f_m + \Theta_m f_{m'}^*) + \beta_T^2(\Theta_{m'}^* \Theta_m'' - \Theta_m \Theta_{m'}''^*) + \frac{\beta_T^2}{r}(\Theta_{m'}^* \Theta_m' - \Theta_{m'}'^* \Theta_m) + \frac{in}{r}(\beta_L^2 - \beta_T^2)[\Theta_{m'}^* R_m' + \Theta_m R_{m'}'^*]. \tag{A4}$$

Summation of equations (A3) and (A4) provides:

$$(\omega_m^2 - \omega_{m'}^2)[R_{m'}^* R_m + \Theta_{m'}^* \Theta_m] = \frac{in\alpha}{\rho r}[\Theta_{m'}^* f_m + \Theta_m f_{m'}^*] + \frac{\alpha}{\rho}(R_{m'}^* f_m' - R_m f_{m'}'^*) + \frac{\beta_L^2}{r}\frac{d}{dr}[r(R_m' R_{m'}^* - R_m R_{m'}'^*)] + \frac{\beta_L^2}{r}\frac{d}{dr}[r(\Theta_m' \Theta_{m'}^* - \Theta_m \Theta_{m'}'^*)] + (\beta_L^2 - \beta_T^2)\frac{in}{r}\frac{d}{dr}[R_{m'}^* \Theta_m + R_m \Theta_{m'}^*]. \tag{A5}$$

From equation (2), applying equation (A2), we obtain:

$$f_m'' + \frac{1}{r}f_m' - \frac{n^2}{r^2}f_m = \frac{4\pi\alpha}{\epsilon_\infty}\left[\frac{1}{r}R_m + R_m' + \frac{in}{r}\Theta_m\right]. \tag{A6}$$

From equation (A6), after straightforward mathematical manipulations, we can find that:

$$\frac{in\alpha}{\rho r}[\Theta_m f_{m'}^* + \Theta_{m'}^* f_m] = \frac{\epsilon_\infty}{4\pi\alpha}\left[(f_m'' f_{m'}^* - f_{m'}''^* f_m) + \frac{1}{r}(f_m' f_{m'}^* - f_{m'}'^* f_m)\right] + \frac{\alpha}{\rho r}[R_m f_{m'}^* - f_m R_{m'}^*] - \frac{\alpha}{\rho}[R_m' f_{m'}^* - R_{m'}'^* f_m]. \tag{A7}$$

Substitution of equation (A7) into equation (A5) leads us to:

$$(\omega_m^2 - \omega_{m'}^2)(R_{m'}^* R_m + \Theta_{m'}^* \Theta_m) = \frac{\epsilon_\infty}{4\pi\alpha}\frac{1}{r}\frac{d}{dr}[r(f_m' f_{m'}^* - f_{m'}'^* f_m)] + \frac{\alpha}{\rho}\frac{1}{r}\frac{d}{dr}[r(R_{m'}^* f_m - R_m f_{m'}^*)] + \frac{\beta_L^2}{r}\frac{d}{dr}[r(\Theta_m' \Theta_{m'}^* - \Theta_m \Theta_{m'}'^*)] + (\beta_L^2 - \beta_T^2)\frac{in}{r}\frac{d}{dr}[R_{m'}^* \Theta_m + R_m \Theta_{m'}^*]. \tag{A8}$$

Integration of equation (A8) gives:

$$(\omega_m^2 - \omega_{m'}^2)\int_0^{r_0}[R_{m'}^* R_m + \Theta_{m'}^* \Theta_m] r\,dr = \frac{\epsilon_\infty r_0}{4\pi\alpha}(f_m' f_{m'}^* - f_{m'}'^* f_m)|_{r=r_0} + (\beta_L^2 - \beta_T^2)in[R_{m'}^* \Theta_m + R_m \Theta_{m'}^*]|_{r=0}. \tag{A9}$$

It is easy to prove that $u_{nm} = 0$ for $r = 0$ whenever $n \neq 1$. But for $n = 1$ it is seen that:

$$[R^*_{m'}\Theta_m + R_m\Theta^*_{m'}]|_{r=0} = 0.$$

On the other hand, due to matching boundary conditions, it is seen that the first term on the right-hand side of equation (A9) is zero. Hence, we have proven that, for $m \neq m'$:

$$\int_0^{r_0} [R^*_{m'}R_m + \Theta^*_{m'}\Theta_m]r\,dr = 0. \tag{A10}$$

This is the orthogonality condition for our present problem, valid for both the QW and the FSW.

References

[1] Klein M V 1986 *IEEE, J. Quantum Electron.* **QE-22** 1760
[2] Sood A K, Menéndez J, Cardona M and Ploog K 1985 *Phys. Rev. Lett.* **54** 2111
[3] Cardona M and Güntherodt G (ed) 1989 *Light Scattering in Solids V (Springer Topics in Applied Physics 66)* (Heidelberg: Springer)
[4] Mowbray D J, Cardona M and Ploog K 1991 *Phys. Rev.* B **43** 11 815
[5] Pokatilov E P and Beril S E 1983 *Phys. Status Solidi* b **118** 567
Fomin V M and Pokatitov E P 1985 *Phys. Status Solidi* b **132** 69
[6] Bechstedt F and Enderlain R 1985 *Phys. Stat. Solidi* b **131** 53
[7] Mori N and Ando T 1989 *Phys. Rev.* B **40** 6175
[8] Nash K J 1992 *Phys. Rev.* B **46** 7723
[9] Weber G 1992 *Phys. Rev.* B **46** 16 171
[10] Babiker M 1986 *J. Phys. C: Solid State Phys.* **19** 683
[11] Wendler L 1985 *Phys. Status Solidi* b **129** 513
Wendler L and Haupt R 1987 *Phys. Status Solidi* b **143** 487
[12] Cher R, Lin D L and Geroge T F 1990 *Phys. Rev.* B **41** 1435
[13] Trallero-Giner C and Comas F 1988 *Phys. Rev.* B **37** 4583
[14] Cardona M 1990 *Superlatt. Microstruct.* **7** 183
[15] Rucker H, Molinari E and Lugli P 1991 *Phys. Rev.* B **44** 3463; 1992 *Phys. Rev.* B **45** 6747
Molinari E, Fasolino A and Kunc K 1986 *Superlatt. Microstruct.* **2** 393
Molinari E, Baroni S, Giannozi P and de Gironcoli S 1992 *Phys. Rev.* B **45** 4280
[16] Huang K and Zhu B 1988 *Phys. Rev.* B **38** 13 377
[17] Ridley B K 1993 *Phys. Rev.* B **47** 4592; 1991 *Phys. Rev.* B **44** 9002
[18] Akera H and Ando T 1989 *Phys. Rev.* B **40** 2914
[19] Richter E and Strauch D 1987 *Solid. State Commun.* **64** 867
[20] Ren S F, Chu H Y and Chang C Y 1988 *Phys. Rev.* B **37** 8899
[21] Bechstedt F and Gerecke H 1989 *Phys. Status Solidi* b **156** 151
[22] Comas F, Pérez R, Trallero-Giner C and Cardona M, 1994 *Superlatt. Microstruct.* **14** 95
Perez-Alvarez R, García Moliner F, Velasco V R and Trallero-Giner C 1993 *J. Phys. C: Solid State Phys.* **5** 5389
[23] Chamberlain M P, Cardona M and Ridley B K 1993 *Phys. Rev.* B **48** 14 356
[24] Trallero-Giner C, Garcia-Moliner F, Velasco V R and Cardona M 1992 *Phys. Rev.* B **45** 11 944
[25] Comas F, Trallero-Giner C and Cantarero A 1993 *Phys. Rev.* B **47** 7602
(see also 'Phonons in Semiconductor Nanostructures' 1993 *NATO ASI Series E 236* ed J P Leburton, J Pascual and C Sotomayor Torres (Dordrecht: Kluwer) p 49)
[26] Stroscio M A 1989 *Phys. Rev.* B **40** 6428
[27] Constantinou N and Ridley B K 1990 *Phys. Rev.* B **41** 10 622, 10 627
[28] Stroscio M A, Kim K W, Littlejohn M A and Chuang H 1990 *Phys. Rev.* B **42** 1488
[29] Knipp P A and Reinecke T L 1992 *Phys. Rev.* B **45** 9091; 1993 *Phys. Rev.* B **48** 5700
[30] Enderlein R 1993 *Phys. Rev.* B **47** 2162
[31] Watt M, Sotomayor-Torres C M, Arnot H E G and Beaumont S P 1990 *Semicond. Sci. Technol.* **5** 285
[32] Ren S F and Chang Y C 1991 *Phys. Rev.* B **43** 11 857
[33] Kim K W, Stroscio M A, Bhatt A, Mickevicius R and Mitin V V 1991 *J. Appl. Phys.* **70** 319

[34] Zhu B 1991 *Phys. Rev.* B **44** 1926
[35] Wang X F and Lei X L 1994 *Phys. Rev.* B **49** 4780
[36] Rossi F, Rota L, Bungaro C, Lugli P and Molinari E, 1993 *Phys. Rev.* B **47** 1695
[37] Jusserand B and Cardona M 1989 *Light Scattering in Solids V (Springer Topics in Applied Physics 66)* ed M Cardona and G Güntherodt (Heidelberg: Springer) p 61
[38] It should be noted that in [25] there is a misprint in the expression for ϕ. The correct expression is given by (22) of the present work.
[39] Trallero-Giner C, Comas F and García-Moliner F 1994 *Phys. Rev.* B **50** 1755
[40] Fröhlich H 1948 *Theory of Dielectrics* (Oxford: Oxford University Press)
[41] Roca E, Trallero-Giner C and Cardona M 1994 *Phys. Rev.* B **49** 13 704